Estimation of fracture parameters from reflection seismic data, Part II: Fractured models with orthorhombic symmetry

Andrey Bakulin*, Vladimir Grechka†, and Ilya Tsvankin†

*Schlumberger Cambridge Research, High Cross, Madingley Road, Cambridge, CB3 0EL, England
(Previous address: Department of Geophysics, St.-Petersburg State University, St. Petersburg, Russia)
† Center for Wave Phenomena

ABSTRACT

Existing geophysical and geological data indicate that orthorhombic media with a horizontal symmetry plane should be rather typical for naturally fractured reservoirs. Here, we consider two orthorhombic models, one of which contains parallel vertical fractures embedded in a transversely isotropic background with a vertical symmetry axis (VTI medium), and the other is due to two orthogonal sets of rotationally invariant fractures in a purely isotropic host rock.

Using the linear slip theory of Schoenberg, we obtain simple analytic expressions for the anisotropic coefficients of the effective orthorhombic media. Under the assumptions of weak anisotropy of the background medium and small compliances of the fractures, all effective anisotropic parameters reduce to the sum of the background values and the parameters due to each fracture set. For the model with a single fracture system, this result allows us to eliminate the influence of the VTI background by evaluating the differences between the anisotropic parameters defined in the vertical symmetry planes. Then the dimensionless fracture weaknesses, which carry information about both the density and content of the fracture network, can be determined in the same way as for fracture-induced HTI (transversely isotropic with a horizontal symmetry axis) media examined in our previous paper (Part I). The parameter-estimation procedure can be based on the azimuthally-dependent reflection traveltimes and prestack amplitudes of P-waves alone, if an estimate of the ratio of the P- and S-wave vertical velocities is available.

In each vertical symmetry plane of the model with two orthogonal fracture sets, the anisotropic parameters are largely governed by the weaknesses of the fractures orthogonal to this plane. Therefore, for weakly anisotropic media the fracture sets are essentially decoupled, and their parameters can be estimated by means of two independently performed HTI inversions. It is crucial that the input data for this model include the vertical velocities (or reflector depth) because it is necessary to resolve the anisotropic coefficients in each vertical symmetry plane rather than their differences.

We also discuss several criteria which can be used to distinguish between the models with one and two fracture sets. For example, the semi-major axis of the P-wave NMO ellipse and the polarization direction of the vertically traveling fast shear wave are always parallel to each other for a single system of fractures but may become orthogonal in the medium with two fracture sets.

Introduction

Characterization of fractured reservoirs using surface seismic data continues to be a topic of significant exploration interest. A number of publications, both theoretical and experimental, were devoted to the processing and inversion of seismic data acquired over azimuthally anisotropic fractured formations (e.g., Martin and Davis, 1987; Mueller, 1991; Lynn et al., 1996; Rüger and Tsvan-

kin, 1997; Withers and Corrigan, 1997; Tsvankin, 1997a; Grechka and Tsvankin, 1999a). Fracture-detection algorithms discussed in the literature are largely aimed at estimating the fracture orientation (under the assumption of a single fracture system) and evaluating seismic attributes that would provide a measure of relative fracture intensity over the survey area. More quantitative inversion methods for azimuthally anisotropic media (e.g., Grechka and Tsvankin, 1999a; Grechka et al., 1999) are designed to obtain a certain subset of the anisotropic parameters of the effective medium. Further interpretation of the inversion results in terms of the physical properties of fracture networks requires application of effective models of fracture media, such as those developed by Schoenberg (1980, 1983), Hudson (1980, 1981, 1988) and Thomsen (1995).

This is the second paper of our series of three publications on seismic fracture characterization. The main goal of the series is to provide a connection between seismic fracture-detection methods and rock-physics models of fractured media. In particular, we are interested in elucidating the dependence of reflection seismic signatures on the physical parameters of the fractures and developing inversion algorithms for estimating fracture parameters using P and converted (PS) reflection data. In the first paper of the series (Bakulin et al., 1999; hereafter referred to as Paper I) we addressed these problems for the simplest azimuthally anisotropic model – transverse isotropy with a horizontal axis of symmetry (HTI media).

The HTI model describes a single set of vertical, parallel, rotationally invariant fractures in a purely isotropic background medium. As discussed in Paper I, the fracture orientation and the so-called fracture compliances (or weaknesses) introduced in the linear slip theory of Schoenberg (1980, 1983) are the only quantities constrained by seismic data acquired over HTI formations. A more detailed information about the fractures including their shape and degree of saturation is beyond the capabilities of seismic methods, unless specific assumptions about the fracture microstructure are made. For instance, if the cracks are known to be penny-shaped (i.e., they have the shape of oblate spheroids) and isolated from pore space, it is possible to evaluate both the crack density and fluid saturation using seismic data. Paper I describes several possible ways of inverting normal-moveout (NMO) velocities and reflection coefficients of P- and PS-waves for the normal and tangential compliances of the fractures. If the ratio of the vertical P and S-wave velocities is known, P-wave data alone can be used to estimate the crack density and distinguish between dry and fluid-filled cracks.

However, since the rock matrix of most subsurface formations exhibits some form of anisotropy, it is difficult to expect that the HTI model can give an adequate description of typical fractured reservoirs. Here, we extend the approach of Paper I to more complicated, but likely more realistic, orthorhombic models. The description of seismic signatures in orthorhombic media can be significantly simplified by using Tsvankin's (1997b) notation based on the analogy between the symmetry planes of orthorhombic and transversely isotropic media. For instance, P-wave velocities and traveltimes are fully controlled by the vertical velocity and five dimensionless anisotropic coefficients introduced by Tsvankin (1997b), rather than on nine stiffnesses in the conventional notation. Also, this parameterization yields concise expressions for NMO velocities of pure modes reflected from a horizontal interface (Grechka and Tsvankin, 1998; Grechka et al., 1999). As shown by Grechka et al. (1999), eight out of nine parameters of orthorhombic media with a horizontal symmetry plane can be obtained from the NMO velocities of horizontal P and split PS events, provided the vertical velocities or reflector depth are known. Reflection moveout of P-waves alone is sufficient to find the orientation of the symmetry planes, NMO velocities within them, and three "anellipticity" coefficients η. The parameters η, however, can be obtained only if dipping events or nonhyperbolic moveout are available.

While orthorhombic symmetry may be caused by a variety of physical reasons, in this paper we restrict ourselves to two orthorhombic models believed to be most common for fractured reservoirs: (i) a single set of vertical cracks in a background medium characterized by vertical transverse isotropy (VTI), and (ii) two systems of vertical fractures orthogonal to each other in an isotropic background medium. If both the intrinsic anisotropy of the host rock and the anisotropy induced by the fractures are weak, the anisotropic coefficients of the background and fractures can be algebraically *added* in describing the effective medium. This result provides important insights into the influence of fractures on the effective anisotropy and helps to generalize the parameter-estimation methodology of Paper I for orthorhombic media. For the model with a single fracture set in a VTI background, the azimuthal variation of such seismic signatures as NMO velocity and amplitude-versus-offset (AVO) gradient is largely independent of the properties of the background and can be inverted for the fracture parameters. Also, we introduce practical strategies to invert the signatures of P- and PS-waves for the physical parameters of the medium with two fracture systems.

One set of vertical fractures in a VTI background

Effective orthorhombic medium

A single system of vertical fractures embedded in a VTI matrix yields an effective medium of orthorhombic symmetry. According to the linear slip theory developed by Schoenberg (1980, 1983),* the effective compliance tensor of such a medium can be obtained by simply adding the excess fracture compliances to the compliance of the background. The inversion of the resulting compliance tensor yields the stiffness tensor (and the corresponding two-index stiffness matrix) of the fracture-induced orthorhombic model. If the fracture faces are perpendicular to the x_1-axis, the effective stiffness matrix $\mathbf{c}$ has the following form (Schoenberg and Helbig, 1997; Appendix A):

$$\mathbf{c}=\begin{pmatrix} c_{11} & c_{12} & c_{13} & 0 & 0 & 0 \\ c_{12} & c_{22} & c_{23} & 0 & 0 & 0 \\ c_{13} & c_{23} & c_{33} & 0 & 0 & 0 \\ 0 & 0 & 0 & c_{44} & 0 & 0 \\ 0 & 0 & 0 & 0 & c_{55} & 0 \\ 0 & 0 & 0 & 0 & 0 & c_{66} \end{pmatrix} = \left(\begin{array}{c|c} \tilde{\mathbf{c}}_1 & \mathbf{0} \\ \hline \mathbf{0} & \tilde{\mathbf{c}}_2 \end{array}\right), \tag{1}$$

where $\tilde{\mathbf{c}}_1$ and $\tilde{\mathbf{c}}_1$ are given by

$$\tilde{\mathbf{c}}_1 = \begin{pmatrix} c_{11b}\,\ell & c_{12b}\,\ell & c_{13b}\,\ell \\ c_{12b}\,\ell & c_{11b}-\wp_1 & c_{13b}-\wp_2 \\ c_{13b}\,\ell & c_{13b}-\wp_2 & c_{33b}-\wp_3 \end{pmatrix}, \tag{2}$$

$$\tilde{\mathbf{c}}_2 = \begin{pmatrix} c_{44b} & 0 & 0 \\ 0 & c_{44b}\,(1-\Delta_V) & 0 \\ 0 & 0 & c_{66b}\,(1-\Delta_H) \end{pmatrix}, \tag{3}$$

$\ell = 1-\Delta_N$, $\wp_1 = \Delta_N\, c_{12b}^2/c_{11b}$, $\wp_2 = \Delta_N\, c_{12b}\, c_{13b}/c_{11b}$, $\wp_3 = \Delta_N\, c_{13b}^2/c_{11b}$, and $\mathbf{0}$ is the 3×3 zero matrix. c_{ij_b} are the stiffness coefficients of the VTI background (constrained by $c_{12b} = c_{11b} - 2\,c_{66b}$), and Δ_N, Δ_V, and Δ_H are the dimensionless weaknesses (Schoenberg and Helbig, 1997; Bakulin and Molotkov, 1998) that characterize the intensity of fracturing and change from zero (no fractures) to unity (extreme fracturing). The tangential weaknesses Δ_V and Δ_H provide a measure of crack density whereas the normal weakness Δ_N contains information about the fluid content of the fractures and possible fluid flow between the fractures and pore space (Schoenberg and Douma, 1988; Paper I).

The matrix (1) describes a special type of orthorhombic media with the stiffnesses satisfying the relation (Schoenberg and Helbig, 1997)

$$c_{13}\,(c_{22}+c_{12}) = c_{23}\,(c_{11}+c_{12}). \tag{4}$$

The existence of the additional constraint (4) stems from the fact that while general orthorhombic media are characterized by nine independent c_{ij}'s, the fracture-induced model considered here is defined by only eight quantities: five stiffness coefficients c_{11b}, c_{13b}, c_{33b}, c_{44b}, and c_{66b} of the VTI background and three fracture weaknesses Δ_N, Δ_V, and Δ_H.

Weak-anisotropy approximation

The inversion of surface data for the physical parameters of the fractures requires relating seismic signatures to the fracture weaknesses Δ_N, Δ_V and Δ_H. The results of Grechka and Tsvankin (1999b) and Grechka et al. (1999) show that in orthorhombic media such commonly used signatures as NMO velocities and AVO gradients are most concisely expressed through the dimensionless anisotropic coefficients introduced by Tsvankin (1997b). The definitions of Tsvankin's parameters $\epsilon^{(1,2)}$, $\delta^{(1,2,3)}$ and $\gamma^{(1,2)}$ in terms of the stiffness elements c_{ij} are given in Appendix B. Substituting equations (1)–(3) for the stiffnesses of the fracture-induced orthorhombic model yields the anisotropic coefficients ϵ, δ and γ as functions of the weaknesses Δ_N, Δ_V, and Δ_H.

These exact expressions, however, are too complicated to give an insight into the influence of the fractures on the effective anisotropic model. Therefore, here we assume that Thomsen's (1986) anisotropic coefficients ϵ_b, δ_b, and γ_b in the VTI background, along with the weaknesses Δ_N, Δ_V, and Δ_H, are small quantities of the same order. Linearization of the effective stiffness matrix in the anisotropic parameters leads to equation (A17) showing that for weak anisotropy the effective anisotropic coefficients $\epsilon^{(1,2)}$, $\delta^{(1,2,3)}$, and $\gamma^{(1,2)}$ should represent the *sums* of the VTI background parameters ϵ_b, δ_b, and γ_b and the corresponding anisotropic coefficients of the HTI medium due to the fractures in an imaginary *isotropic* host rock sufficiently close to the VTI background model. This isotropic medium can be characterized, for instance, by the P- and S-wave velocities V_P and V_S equal to the vertical velocities V_{P0b} and V_{S0b} in the VTI background.

Since this result provides a theoretical underpinning for most of the subsequent discussion, we prove it for one of the anisotropic coefficients – the parameter $\epsilon^{(2)}$ defined by equation (B3). Substituting the stiffnesses from equations (1) and (2) into (B3) yields

* Comparison of the linear slip theory with the effective media theories of Hudson (1980; 1981; 1988) and Thomsen (1995) can be found in Paper I.

$$\epsilon^{(2)} = \frac{c_{11\,b} - c_{33\,b} - \Delta_N \left(c_{11\,b} - \frac{c_{13\,b}^2}{c_{11\,b}} \right)}{2\, c_{33\,b} \left(1 - \Delta_N \frac{c_{13\,b}^2}{c_{11\,b} c_{33\,b}} \right)} . \tag{5}$$

Using the definition of the coefficient ϵ_b in the VTI background medium ($\epsilon_b \equiv \frac{c_{11\,b} - c_{33\,b}}{2\, c_{33\,b}}$; see Thomsen, 1986), equation (5) can be rewritten as

$$\epsilon^{(2)} = \frac{\epsilon_b - \Delta_N \frac{c_{11\,b}^2 - c_{13\,b}^2}{2\, c_{11\,b}\, c_{33\,b}}}{1 - \Delta_N \frac{c_{13\,b}^2}{c_{11\,b}\, c_{33\,b}}} . \tag{6}$$

Linearizing this equation with respect to ϵ_b and Δ_N, we drop the anisotropic term in the denominator to obtain

$$\epsilon^{(2)} \approx \epsilon_b - \Delta_N \frac{c_{11\,b}^2 - c_{13\,b}^2}{2\, c_{11\,b}\, c_{33\,b}} . \tag{7}$$

Since the fraction $\frac{c_{11\,b}^2 - c_{13\,b}^2}{c_{11\,b}\, c_{33\,b}}$ is multiplied by the already small weakness Δ_N, it can be replaced in the weak anisotropy approximation by the corresponding isotropic quantity $4\, g\, (1 - g)$, where $g \equiv V_{S0b}^2 / V_{P0b}^2$ is the ratio of the squared vertical S- and P-wave velocities in the background. This allows us to represent equation (7) as

$$\epsilon^{(2)} \approx \epsilon_b - 2\, g\, (1 - g)\, \Delta_N . \tag{8}$$

The combination $-2\, g\, (1 - g)\, \Delta_N$ can be recognized as the linearization of the anisotropic coefficient $\epsilon^{(\mathrm{V})}$ (Rüger, 1997; Tsvankin, 1997a) in an HTI medium due a single set of vertical fractures embedded in a purely isotropic rock with the squared S-to-P velocity ratio g (Paper I). Hence, equation (8) implies that

$$\epsilon^{(2)} \approx \epsilon_b + \epsilon^{(\mathrm{V})} . \tag{9}$$

We conclude that in the weak-anisotropy limit the anisotropic coefficient $\epsilon^{(2)}$ reduces to the sum of the Thomsen background parameter ϵ_b and the coefficient $\epsilon^{(\mathrm{V})}$ of the HTI model due to the fractures embedded in an isotropic medium "close enough" to the VTI background medium. Similar linearizations for the other anisotropic parameters of the effective orthorhombic model are given below.

Symmetry plane $[x_2, x_3]$ parallel to the fractures
The linearized anisotropic coefficients in the symmetry plane $[x_2, x_3]$, derived from equations (B6)–(B8), have the following form:

$$\epsilon^{(1)} = \epsilon_b , \tag{10}$$

$$\delta^{(1)} = \delta_b , \tag{11}$$

and

$$\gamma^{(1)} = \gamma_b + \frac{\Delta_V - \Delta_H}{2} . \tag{12}$$

Therefore, in the weak-anisotropy limit the coefficients $\epsilon^{(1)}$ and $\delta^{(1)}$ coincide with those of the VTI background medium. This is an expected result because if rotationally invariant fractures are introduced into an isotropic matrix, the plane $[x_2, x_3]$ represents the so-called isotropy plane of the effective HTI medium. In the isotropy plane the velocities of all waves are not influenced by the fractures and remain constant for all propagation directions (e.g., Tsvankin, 1997a). The coefficient $\gamma^{(1)}$ is different from γ_b only because, in contrast to the more conventional model from Paper I, the fractures considered here are not rotationally invariant (i.e., $\Delta_V \neq \Delta_H$).

In addition to the basic set of the anisotropic parameters introduced by Tsvankin (1997b), it is useful to consider the "anellipticity" coefficients $\eta^{(1,2,3)}$ responsible for time processing of P-wave data (Grechka and Tsvankin, 1999b). For weak anisotropy, the η coefficient in the $[x_2, x_3]$-plane given by equation (B10) is also equal to the background value:

$$\eta^{(1)} = \eta_b . \tag{13}$$

Symmetry plane $[x_1, x_3]$ perpendicular to the fractures
The weak-anisotropy approximations of the anisotropic coefficients in the plane $[x_1, x_3]$ are given by as follows:

$$\epsilon^{(2)} = \epsilon_b - 2\, g\, (1 - g)\, \Delta_N , \tag{14}$$

$$\delta^{(2)} = \delta_b - 2\, g\, [(1 - 2g) \Delta_N + \Delta_V] , \tag{15}$$

$$\gamma^{(2)} = \gamma_b - \frac{\Delta_H}{2} , \tag{16}$$

$$\eta^{(2)} = \eta_b + 2\, g\, [\Delta_V - g\, \Delta_N] . \tag{17}$$

Each of the expressions (14)–(17) contains two terms with a distinctly different physical meaning. The first term is simply the corresponding anisotropic coefficient of the VTI background, while the second term absorbs the influence of the fractures. As discussed above for the parameter $\epsilon^{(2)}$, the fracture-related terms coincide with the coefficients $\epsilon^{(V)}$, $\delta^{(V)}$, $\gamma^{(V)}$, and $\eta^{(V)}$ derived in Paper I for a fracture set embedded in an isotropic background.

The constraint on the effective stiffnesses (4) leads to an additional relationship between the anisotropic coefficients. In the weak-anisotropy limit, equation (4) can be rewritten as

$$\gamma^{(2)} - \gamma^{(1)} = \frac{1}{4\, g} \left[\delta^{(2)} - \delta^{(1)} - \left(\epsilon^{(2)} - \epsilon^{(1)} \right) \frac{1 - 2g}{1 - g} \right] . \tag{18}$$

It is interesting that the background parameters and the tangential compliance Δ_H have no influence on the constraint (18) that depends only on the *differences* between the anisotropic coefficients in the vertical symmetry planes, i.e., on the parameters $\epsilon^{(V)}$, $\delta^{(V)}$ and $\gamma^{(V)}$. As a result, equation (18) is fully analogous to the constraint given by Tsvankin (1997a) and Paper I for HTI media due to rotationally invariant fractures (i.e., for $\Delta_H = \Delta_V$).

Horizontal symmetry plane $[x_1, x_2]$

The only Tsvankin's (1997b) anisotropic coefficient defined in the horizontal plane is $\delta^{(3)}$ [equation (B9)]. After the linearization, it becomes

$$\delta^{(3)} = 2\,g\,[\Delta_N - \Delta_H]\,. \tag{19}$$

The parameter $\delta^{(3)}$ does not contain any background anisotropic coefficients because $[x_1, x_2]$ is the isotropy plane of the VTI medium. Since $\delta^{(3)}$ is defined with respect to the x_1-axis that is normal to the fractures, equation (19) coincides with the expression for the generic Thomsen coefficient δ obtained for VTI media due to *horizontal* fractures by Schoenberg and Douma (1988).

The linearized anellipticity coefficient $\eta^{(3)}$ [equation (B12)] has the form

$$\eta^{(3)} = 2\,g\,[\Delta_H - g\,\Delta_N]\,. \tag{20}$$

Estimation of fracture parameters

Since we are mostly interested in evaluating the properties of the fracture set, it is convenient to remove the influence of the background medium at the outset of the inversion procedure. Inspection of equations (10)–(17) shows that the contribution of the VTI background parameters can be eliminated by computing the *difference* between the anisotropic coefficients in the planes parallel and orthogonal to the fractures:

$$\epsilon^{(2)} - \epsilon^{(1)} = -2\,g\,(1-g)\,\Delta_N\,, \tag{21}$$

$$\delta^{(2)} - \delta^{(1)} = -2\,g\,[(1-2g)\Delta_N + \Delta_V]\,, \tag{22}$$

$$\gamma^{(2)} - \gamma^{(1)} = -\frac{\Delta_V}{2}, \tag{23}$$

$$\eta^{(2)} - \eta^{(1)} = 2\,g\,[\Delta_V - g\,\Delta_N]\,. \tag{24}$$

Equations (21)–(24) are identical to the expressions for $\epsilon^{(V)}$, $\delta^{(V)}$, $\gamma^{(V)}$, and $\eta^{(V)}$ (respectively) in HTI media due to a single set of vertical rotationally invariant fractures with the weaknesses Δ_N and Δ_V (Paper I). Therefore, the weaknesses can be determined from equations (21)–(24) using the HTI expressions described in detail in Paper I.

Recovery of the anisotropic parameters from surface data

The differences between the anisotropic coefficients defined in the vertical symmetry planes can be obtained from the azimuthal dependence of normal-moveout velocities and AVO gradients. Azimuthally varying NMO velocity of the P-wave in a horizontal orthorhombic layer is described by an ellipse with the semi-axes $V^{(1)}_{P,\mathrm{nmo}}$ and $V^{(2)}_{P,\mathrm{nmo}}$ in the vertical symmetry planes (Grechka and Tsvankin, 1998):

$$V^{(i)}_{P,\mathrm{nmo}} = V_{P0}\sqrt{1+2\,\delta^{(i)}}\,, \qquad (i=1,2)\,. \tag{25}$$

The difference χ between the two δ coefficients [equation (22)] can be evaluated from equations (25) in the following way:

$$\chi = \frac{\left(V^{(2)}_{P,\mathrm{nmo}}\right)^2 - \left(V^{(1)}_{P,\mathrm{nmo}}\right)^2}{\left(V^{(2)}_{P,\mathrm{nmo}}\right)^2 + \left(V^{(1)}_{P,\mathrm{nmo}}\right)^2} = \frac{\delta^{(2)} - \delta^{(1)}}{1+\delta^{(2)}+\delta^{(1)}} \approx \delta^{(2)} - \delta^{(1)}\,, \tag{26}$$

In the orthorhombic model due to a single fracture set, $\delta^{(1)} > \delta^{(2)}$ [equation (22)], and the semi-major axis of the P-wave NMO ellipse points in the direction of the fracture strike. This result holds for horizontal transverse isotropy as well (Paper I).

The values of $\eta^{(2)}$ and $\eta^{(1)}$ (or $\epsilon^{(2)}$ and $\epsilon^{(1)}$) can be obtained using the NMO velocities of P-wave reflections from dipping interfaces (Grechka and Tsvankin, 1999b) or nonhyperbolic moveout in the directions parallel and perpendicular to the fractures (Al-Dajani et al., 1998). Thus, if an estimate of the V_S/V_P ratio (g) is available, P-wave moveout data provide sufficient information to determine the weaknesses Δ_N and Δ_V (explicit expressions are given below).

If the P-wave moveout information is limited to the NMO ellipse of horizontal events, it is possible to obtain the difference $\gamma^{(2)} - \gamma^{(1)}$ by using the P-wave AVO gradients in the directions parallel and perpendicular to the fractures. In the weak-anisotropy approximation, the variation of the P-wave AVO gradient between the vertical symmetry planes is governed by the expression $\delta^{(2)} - \delta^{(1)} - 8\,g\,(\gamma^{(2)} - \gamma^{(1)})$ (Rüger, 1998). If the velocity ratio g is known and $\delta^{(2)} - \delta^{(1)}$ has been found from the P-wave NMO ellipse, the AVO gradient yields an estimate of $\gamma^{(2)} - \gamma^{(1)} = -\Delta_V/2$. The normal weakness Δ_N can then be evaluated from $\delta^{(2)} - \delta^{(1)}$ [equation (22)]. The algorithm based on the NMO ellipses of horizontal events and AVO gradients is identical to the one described in Paper I for HTI media. The presence of anisotropy in the background has no influence either on estimating $\delta^{(2)} - \delta^{(1)}$ and $\gamma^{(2)} - \gamma^{(1)}$ or on inverting these differences for the weaknesses Δ_N and Δ_V.

If shear or converted waves are recorded, their vertical traveltimes (in combination with P-wave data) give a direct estimate of the V_S/V_P ratio g. The difference $\gamma^{(2)} - \gamma^{(1)}$ represents the shear-wave splitting parameter at vertical incidence conventionally determined from the time delays between the fast and slow shear or converted waves. Also, the difference between the AVO gradients of the split converted (PS) can be combined with the azimuthal variation of the P-wave AVO gradient or the P-wave NMO ellipse to obtain another estimate of

$\gamma^{(2)}-\gamma^{(1)}$. A more detailed discussion of the AVO inversion for HTI media is given in Paper I.

Inversion for the weaknesses

While the weaknesses Δ_N and Δ_V can be obtained from the differences in the anisotropic parameters using the HTI expressions of Paper I, the remaining weakness Δ_H has to be discussed separately. Note that Δ_H does not enter any of the differences (21)–(24) despite the fact that it appears in the equations (12) and (16) for $\gamma^{(1)}$ and $\gamma^{(2)}$. However, even if the coefficients $\gamma^{(1)}$ and $\gamma^{(2)}$ were determined separately, they constrain only the combination $\gamma_b - \Delta_H/2$ that contains the unknown background coefficient γ_b. Therefore, the only source of information about the weakness Δ_H is the parameter $\eta^{(3)}$ or $\delta^{(3)}$ [equations (19) and (20)], which can be estimated using the NMO velocities of P-wave reflections from dipping interfaces (Grechka and Tsvankin, 1999b).

If such reflections are not available, a reasonable simplifying assumption is that the fractures are rotationally invariant, and $\Delta_V = \Delta_H$. Then the number of independent medium parameters reduces to seven, and the coefficients $\delta^{(3)}$ and $\eta^{(3)}$ can be expressed as

$$\delta^{(3)} = \delta^{(2)} - \delta^{(1)} - 2\,(\epsilon^{(2)} - \epsilon^{(1)})\,, \tag{27}$$

$$\eta^{(3)} = \eta^{(2)} - \eta^{(1)}\,. \tag{28}$$

In the following, we assume that seismic data have been inverted for the differences $\delta^{(2)}-\delta^{(1)}$, $\eta^{(2)}-\eta^{(1)}$ (or $\epsilon^{(2)}-\epsilon^{(1)}$), $\gamma^{(2)}-\gamma^{(1)}$ and the parameter $\eta^{(3)}$. It should be emphasized that determination of the weaknesses Δ_N and Δ_V requires knowledge of any two of the three differences $\delta^{(2)}-\delta^{(1)}$, $\epsilon^{(2)}-\epsilon^{(1)}$ and $\gamma^{(2)}-\gamma^{(1)}$ [if necessary, the remaining one is given by the constraint (18)]. Then the fracture weaknesses can be found, for example, from equations (20), (22) and (24):

$$\Delta_N = -\,\frac{(\delta^{(2)}-\delta^{(1)}) + (\eta^{(2)}-\eta^{(1)})}{2\,g\,(1-g)}\,, \tag{29}$$

$$\Delta_V = \frac{1}{2\,(1-g)} \times \left[\frac{1-2\,g}{g}(\eta^{(2)}-\eta^{(1)}) - (\delta^{(2)}-\delta^{(1)})\right], \tag{30}$$

$$\Delta_H = \frac{\eta^{(3)}}{2\,g} + g\,\Delta_N\,. \tag{31}$$

As discussed above, if the coefficient $\eta^{(3)}$ is unknown, the data cannot be inverted for the weakness Δ_H. Note that in general P-wave moveout data provide not just the difference between $\eta^{(2)}$ and $\eta^{(1)}$, but also the individual values of these coefficients (Grechka and Tsvankin, 1999b; Al-Dajani et al., 1998). Therefore, in addition to substituting $\eta^{(2)}-\eta^{(1)}$ into the equations for the weaknesses, we can use the relation $\eta^{(1)} = \eta_b$ to determine the η coefficient in the background VTI model.

It should be emphasized that non-negligible values of both $\eta^{(1)}$ and $\eta^{(2)}$ help to detect the presence of anisotropy in the background and discriminate between HTI and orthorhombic models. For HTI media, all anisotropic coefficients in one of the symmetry planes should go to zero, but the ϵ, δ and γ parameters (unlike η) are difficult to recover from surface data without known vertical velocities or reflector depth.

Interpretation of the weaknesses in terms of the physical properties of the fractures is discussed in Paper I. For rotationally invariant penny-shaped cracks, the tangential weakness $\Delta_V = \Delta_H$ gives an estimate of the crack density, while the normal weakness Δ_N represents a sensitive, albeit non-unique, indicator of fluid content.

Numerical examples

Although the weak-anisotropy approximations provide a useful insight into the parameter-estimation problem, it is preferable to use the exact equations for actual inversion. In the examples below, we compute the fracture weaknesses Δ_N, Δ_V, Δ_H and the anisotropic coefficient η_b of the background by inverting the values of $\chi = (\delta^{(2)}-\delta^{(1)})/(1+\delta^{(2)}+\delta^{(1)})$, $\eta^{(1)}$, $\eta^{(2)}$, and $\eta^{(3)}$ presumably extracted from seismic data. The goals of this numerical study are to examine the sensitivity of the inverted parameters to errors in the input data and in the parameters of the background medium.

Our non-linear inversion algorithm is based on the equations (1)–(3) for the stiffness elements and on the exact expressions for the anisotropic coefficients given in Appendix B. The weak-anisotropy approximations (13) and (29)–(31) are used only to obtain the initial guesses for the weaknesses and the coefficient η_b. The parameters of the background medium (contained in the exact equations for the anisotropic coefficients) are $\epsilon_b = 0.1$, $\delta_b = 0.2$, $\gamma_b = 0.1$, and $g = V_{S0b}^2/V_{P0b}^2 = 0.25$. The fracture set is defined by the weaknesses $\Delta_N = 0.5$, $\Delta_V = \Delta_H = 0.2$, which approximately correspond to penny-shaped gas-filled cracks (see Paper I).

The inversion results are displayed in Figure 1. For the correct input parameters the inversion algorithm produces accurate values of the weaknesses and η_b. Errors in the measured anisotropic parameters of up to ± 0.1 result in similar (often smaller) errors in the inverted values, so the parameter-estimation procedure is reasonably stable. As expected from the analytic results, different inverted parameters are most sensitive to errors in different measured quantities. For example, errors in the parameter χ produce comparable distortions in all three weaknesses reaching ± 0.1 (Figure 1a). The anellipticity coefficient

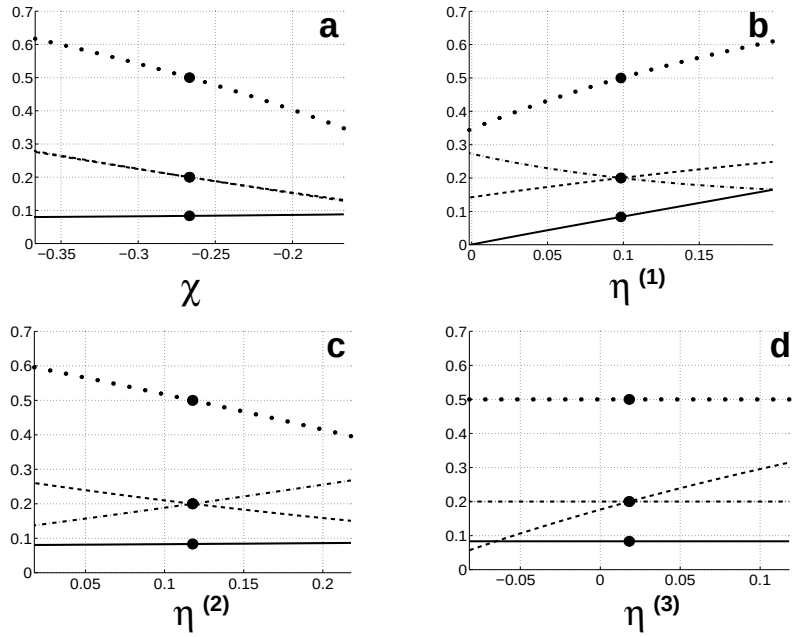

Figure 1. Numerical inversion of $\chi = (\delta^{(2)} - \delta^{(1)})/(1 + \delta^{(2)} + \delta^{(1)})$, $\eta^{(1)}$, $\eta^{(2)}$, and $\eta^{(3)}$ for the fracture weaknesses Δ_N (dotted line), Δ_V (dash-dotted), Δ_H (dashed), and the coefficient η_b of the background medium (solid line). Errors of ± 0.1 were introduced in χ (a), $\eta^{(1)}$ (b), $\eta^{(2)}$ (c), and $\eta^{(3)}$ (d), with the other input parameters held at the correct values. In the absence of errors, the inversion yields the correct values of the weaknesses and η_b (large dots).

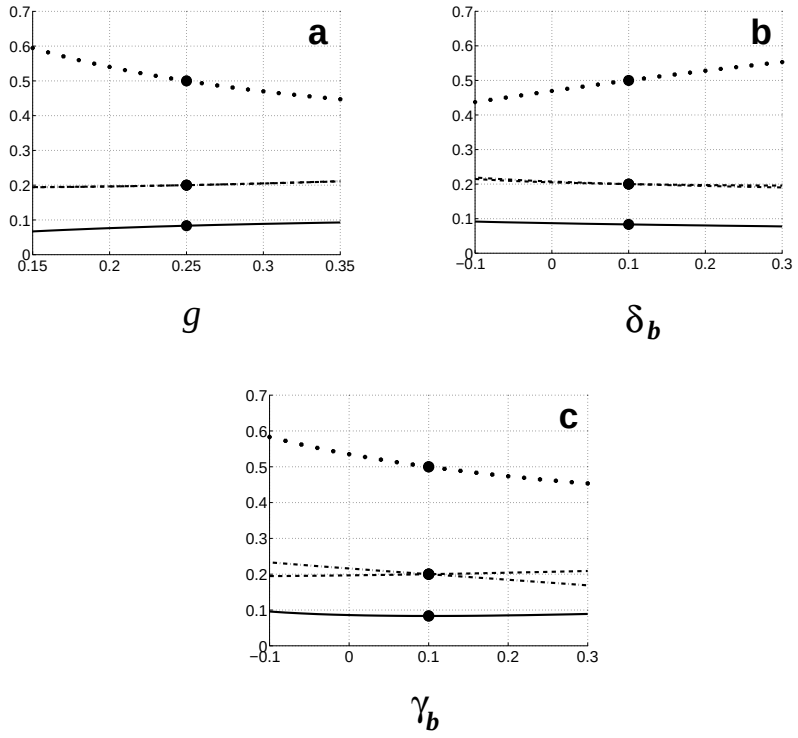

Figure 2. Influence of the background parameters $g = V_{S0b}^2/V_{P0b}^2$ (a), δ_b (b), and γ_b (c) on the numerical inversion results in Figure 1. The dotted line marks Δ_N, dash-dotted – Δ_V, dashed – Δ_H, and solid – η_b.

η_b is quite sensitive to errors in $\eta^{(1)}$ (Figure 1b) and almost independent of the other input parameters in accordance with the weak-anisotropy approximation (13). The errors in $\eta^{(1)}$ and $\eta^{(2)}$ of about ± 0.1 cause smaller errors (± 0.05) in the tangential weaknesses Δ_V and Δ_H than in the normal weakness Δ_N (± 0.1; Figures 1b,c). The weakness Δ_H is sensitive primarily to errors in $\eta^{(3)}$ (Figure 1d), as suggested by equation (31). In the weak anisotropy limit, Δ_N and Δ_V are independent of $\eta^{(3)}$ [equations (29) and (30)], which is confirmed by Figure 1d.

In the second test, we examine the influence of errors in the background parameters g, δ_b, and γ_b (which were assumed known a priori in the previous example) on the inversion results. Although the only background parameter in equations (29)–(31) is the velocity ratio g, the anisotropic coefficients δ_b and γ_b of the VTI medium are contained in the exact equations for the stiffnesses and effective anisotropic parameters. The errors in g of ± 0.1 or less lead to relatively small errors of only about ± 0.03 in all inverted parameters except Δ_N (for Δ_N the errors reach ± 0.1; Figure 2a). The anisotropic coefficients δ_b and γ_b have an even smaller influence on the estimated quantities, especially on the tangential compliances (Figure 2b,c). This result is especially encouraging because the parameters δ_b and γ_b are difficult to estimate from surface seismic data without information about the vertical velocities or reflector depth.

Two orthogonal fracture sets in isotropic rock

Another practically important fractured model with orthorhombic symmetry is composed of two orthogonal fracture sets embedded in an isotropic or VTI background. To simplify the parameter-estimation procedure, we assume that the fractures are rotationally invariant and the background matrix is purely isotropic. Choosing the x_1-axis to be perpendicular to the first set of fractures, we obtain the compliance matrices for both fracture systems in equations (A3) and (A14), where due to the rotational invariance $K_{V1} = K_{H1} \equiv K_{T1}$ and $K_{V2} = K_{H2} \equiv K_{T2}$. Building the effective matrix of the excess compliance [equation (A12)] and adding the compliance of the isotropic background yields the effective stiffness matrix [equation (A1)]

$$\mathbf{c}= \begin{pmatrix} c_{11} & c_{12} & c_{13} & 0 & 0 & 0 \\ c_{12} & c_{22} & c_{23} & 0 & 0 & 0 \\ c_{13} & c_{23} & c_{33} & 0 & 0 & 0 \\ 0 & 0 & 0 & c_{44} & 0 & 0 \\ 0 & 0 & 0 & 0 & c_{55} & 0 \\ 0 & 0 & 0 & 0 & 0 & c_{66} \end{pmatrix}$$

$$= \left(\begin{array}{c|c} \tilde{\tilde{\mathbf{c}}}_1 & \mathbf{0} \\ \hline \mathbf{0} & \tilde{\tilde{\mathbf{c}}}_2 \end{array}\right), \tag{32}$$

where $\mathbf{0}$ is the 3×3 zero matrix, and the matrices $\tilde{\tilde{\mathbf{c}}}_1$ and $\tilde{\tilde{\mathbf{c}}}_2$ are given by

$$\tilde{\tilde{\mathbf{c}}}_1 = \frac{1}{D} \begin{pmatrix} \Lambda\, l_1\, m_3 & \lambda\, l_1\, m_1 & \lambda\, l_1\, m_2 \\ \lambda\, l_1\, m_1 & \Lambda\, l_3\, m_1 & \lambda\, l_2\, m_1 \\ \lambda\, l_1\, m_2 & \lambda\, l_2\, m_1 & \Lambda(l_3\, m_3 - l_4) \end{pmatrix}, \tag{33}$$

$$\tilde{\tilde{\mathbf{c}}}_2 = \tag{34}$$

$$\begin{pmatrix} \mu\,(1-\Delta_{T2}) & 0 & 0 \\ 0 & \mu\,(1-\Delta_{T1}) & 0 \\ 0 & 0 & \mu\,\frac{(1-\Delta_{T1})\,(1-\Delta_{T2})}{1-\Delta_{T1}\,\Delta_{T2}} \end{pmatrix}.$$

Here λ and μ are the Lamé parameters of the background medium, $\Lambda = \lambda + 2\,\mu$, and the coefficients l_i and m_i are expressed as

$$\begin{array}{ll} l_1 = 1 - \Delta_{N1}\,, & l_2 = 1 - r\,\Delta_{N1}\,, \\ l_3 = 1 - r^2\,\Delta_{N1}\,, & l_4 = 4\,r^2\,g^2\,\Delta_{N1}\,\Delta_{N2}\,, \\ m_1 = 1 - \Delta_{N2}\,, & m_2 = 1 - r\,\Delta_{N2}\,, \\ m_3 = 1 - r^2\,\Delta_{N2}\,, & g = \mu/(\lambda+2\mu) = V_S^2/V_P^2\,, \\ r = 1 - 2\,g\,, & D = 1 - r^2\,\Delta_{N1}\,\Delta_{N2}\,. \end{array} \tag{35}$$

Δ_{Ni} and Δ_{Ti} ($i = 1, 2$) are the normal and tangential fracture weaknesses related to the fracture compliances by the equations

$$\Delta_{Ni} = \frac{K_{Ni}\,(\lambda + 2\,\mu)}{1 + K_{Ni}\,(\lambda + 2\,\mu)}\,, \tag{36}$$

$$\Delta_{Ti} = \frac{K_{Ti}\,\mu}{1 + K_{Ti}\,\mu}\,, \tag{37}$$

which represent a special case (valid for an isotropic background) of equations (A4).

Since both fracture planes and the horizontal plane constitute three orthogonal planes of mirror symmetry, the effective medium has to be orthorhombic with the nine independent stiffness elements shown in equation (32). Our model, however, represents a special case of general orthorhombic media with only six independent parameters: λ, μ, Δ_{N1}, Δ_{T1}, Δ_{N2}, and Δ_{T2}. As follows from equations (33) and (34), the three additional relationships (constraints) between the stiffnesses are

$$c_{12}(c_{33} + c_{23}) = c_{13}(c_{22} + c_{23})\,, \tag{38}$$

$$2\,(c_{11} + c_{13}) = \left(c_{11}c_{33} - c_{13}^2\right)\left(\frac{c_{44} + c_{55}}{c_{44}c_{55}} - \frac{1}{c_{66}}\right), \tag{39}$$

and

$$2\,(c_{22} + c_{23}) = \left(c_{22}c_{33} - c_{23}^2\right)\left(\frac{c_{44} + c_{55}}{c_{44}c_{55}} - \frac{1}{c_{66}}\right). \tag{40}$$

Models with two *identical* orthogonal fracture sets, characterized by fewer independent parameters, are discussed in Appendix C.

Anisotropic coefficients in the weak anisotropy limit

Equations (32)–(35), combined with the definitions from Appendix B, can be used to express Tsvankin's (1997b) anisotropic coefficients in terms of the fracture weaknesses Δ_{Ti} and Δ_{Ni}. Here we restrict ourselves to the corresponding linearized expressions obtained in the limit of small fracture compliances $\Delta_{T1,2} \ll 1$ and $\Delta_{N1,2} \ll 1$. The result of this linearization can be predicted from equation (A13): since in the linear approximation fracture systems are not influenced by each other, the effective orthorhombic medium is composed of two HTI media produced by both fracture sets individually.

Symmetry plane $[x_2, x_3]$

The anisotropic parameters with the subscript "(1)" are defined in the symmetry plane $[x_2, x_3]$, which is parallel to the first set of fractures and orthogonal to the second one. In the absence of the second set, the $[x_2, x_3]$-plane would coincide with the isotropy plane of the HTI medium caused by the first fracture system. Therefore, we can expect these parameters to be largely influenced by the second set of fractures which is orthogonal to the x_2-axis. Indeed, the linearized ϵ, δ, γ and η coefficients in the $[x_2, x_3]$ plane depend only on the weaknesses Δ_{N2} and Δ_{T2}:

$$\epsilon^{(1)} = -2\,g\,(1-g)\,\Delta_{N2}\,, \tag{41}$$

$$\delta^{(1)} = -2\,g\,[(1-2\,g)\,\Delta_{N2} + \Delta_{T2}]\,, \tag{42}$$

$$\gamma^{(1)} = -\,\frac{\Delta_{T2}}{2}\,, \tag{43}$$

$$\eta^{(1)} = 2\,g\,[\Delta_{T2} - g\,\Delta_{N2}]\,, \tag{44}$$

where $g \equiv V_S^2/V_P^2$ is the ratio of the squared S- and P-wave velocities in the background.

Symmetry plane $[x_1, x_3]$

Likewise, the linearized anisotropic coefficients in the symmetry plane $[x_1, x_3]$ are governed by the weaknesses of the first fracture set. As follows from the symmetry of the model, the expressions for the parameters $\epsilon^{(2)}$, $\delta^{(2)}$, $\gamma^{(2)}$ and $\eta^{(2)}$ are fully analogous to equations (41)–(44):

$$\epsilon^{(2)} = -2\,g\,(1-g)\,\Delta_{N1}\,, \tag{45}$$

$$\delta^{(2)} = -2\,g\,[(1-2\,g)\,\Delta_{N1} + \Delta_{T1}]\,, \tag{46}$$

$$\gamma^{(2)} = -\,\frac{\Delta_{T1}}{2}\,, \tag{47}$$

and

$$\eta^{(2)} = 2\,g\,[\Delta_{T1} - g\,\Delta_{N1}]\,. \tag{48}$$

Symmetry plane $[x_1, x_2]$

The remaining anisotropic coefficient $\delta^{(3)}$ defined in the horizontal symmetry plane $[x_1, x_2]$ is given by

$$\delta^{(3)} = 2\,g\,[\Delta_{N1} - \Delta_{T1}] - 2\,g\,[(1-2\,g)\,\Delta_{N2} + \Delta_{T2}]\,. \tag{49}$$

The linearized parameter $\delta^{(3)}$ is equal to the sum of the generic Thomsen coefficient δ caused by horizontal fractures (the first term; see Schoenberg and Douma, 1988) and the HTI coefficient $\delta^{(V)}$ due to vertical fractures (Paper I). To explain this result, recall that $\delta^{(3)}$ is defined with respect to the x_1-axis that is orthogonal to the first fracture set (so this set becomes "horizontal") and lies in the planes of the second set of fractures (making this set "vertical").

The anellipticity coefficient $\eta^{(3)}$ [equation (B12)] in the horizontal plane is

$$\eta^{(3)} = \eta^{(1)} + \eta^{(2)}\,. \tag{50}$$

Relations between the anisotropic coefficients

The nine stiffnesses of the orthorhombic model due to two orthogonal fracture sets contain only six independent quantities (λ and μ of the background and the fracture weaknesses Δ_{N1}, Δ_{T1}, Δ_{N2}, and Δ_{T2}), which leads to the three relationships (38)–(40) between the c_{ij}'s. Rewriting the constraints (38) and (39) through Tsvankin's (1997b) parameters yields

$$\gamma^{(i)} = \frac{1}{4\,g}\,\left[\delta^{(i)} - \epsilon^{(i)}\,\frac{1-2\,g}{1-g}\right], \qquad (i=1,2)\,, \tag{51}$$

where quadratic and higher-order terms in the anisotropic coefficients were dropped. The same result can be obtained from the linearized expressions for the anisotropic coefficients in terms of the weaknesses given above. Equation (51) is identical to the relationship between $\epsilon^{(V)}$, $\delta^{(V)}$ and $\gamma^{(V)}$ in HTI media (Tsvankin, 1997a; Paper I).

The remaining constraint (40) takes the form

$$\delta^{(3)} = \delta^{(1)} + \delta^{(2)} - 2\,\epsilon^{(2)}\,. \tag{52}$$

Equations (51) and (52) show that in Tsvankin's notation our orthorhombic model can be fully described by the two vertical velocities and four anisotropic coefficients $\delta^{(1,2)}$ and $\epsilon^{(1,2)}$.

In the special case of penny-shaped gas-filled fractures, the normal and tangential compliances are equal to each other ($K_{N1} = K_{T1}$ and $K_{N2} = K_{T2}$), and, as noticed by Schoenberg and Sayers (1995), the anellipticity parameters in the symmetry planes go to zero:

$$\eta^{(1)} = \eta^{(2)} = \eta^{(3)} = 0\,. \tag{53}$$

Estimation of fracture parameters

The structure of equations (41)–(48) for the anisotropic

coefficients suggests that estimation of the weaknesses of the orthogonal fracture sets can be decomposed into two HTI-type inversions in the vertical symmetry planes discussed in Paper I. Here, we verify the accuracy of the weak-anisotropy approximations given above and outline two possible strategies for obtaining the weaknesses from surface reflection data. One is based on azimuthally dependent P-wave reflection moveout, while the other uses both P- and converted-wave data.

P-wave traveltimes

The axes of the P-wave NMO ellipse in a horizontal orthorhombic layer are always confined to the vertical symmetry planes, which for our model coincide with the fracture planes. Therefore, the fracture orientation can be determined directly from conventional-spread P-wave moveout recorded over a wide range of azimuths, unless the NMO ellipse degenerates into a circle. This and some other special cases are discussed in detail in Appendix D. Even if the P-wave NMO velocity from a horizontal reflector is independent of azimuth, the fracture orientation and the anellipticity coefficients $\eta^{(1)}$, $\eta^{(2)}$, and $\eta^{(3)} \approx \eta^{(1)} + \eta^{(2)}$ [equation (50)] can be obtained from the NMO ellipse of a dipping event (Grechka and Tsvankin, 1999b) or from the azimuthal variation of nonhyperbolic moveout (Al-Dajani et al., 1998).

Suppose the parameters $\delta^{(1)}$ and $\delta^{(2)}$ have been found using the semi-axes of the P-wave NMO ellipse from a horizontal reflector and the vertical velocity [see equations (25)]. Combining the δ coefficients with the anellipticity parameters $\eta^{(1)}$ and $\eta^{(2)}$ allows us to solve equations (42), (44), (46), and (48) for the weaknesses:

$$\Delta_{N1} = -\frac{\delta^{(2)} + \eta^{(2)}}{2\,g\,(1-g)}\,, \tag{54}$$

$$\Delta_{T1} = \frac{1}{2\,(1-g)}\left[\frac{1-2g}{g}\,\eta^{(2)} - \delta^{(2)}\right]\,, \tag{55}$$

$$\Delta_{N2} = -\frac{\delta^{(1)} + \eta^{(1)}}{2\,g\,(1-g)}\,, \tag{56}$$

and

$$\Delta_{T2} = \frac{1}{2\,(1-g)}\left[\frac{1-2g}{g}\,\eta^{(1)} - \delta^{(1)}\right]\,. \tag{57}$$

Note that the equations for each pair of weaknesses [(54)–(55) and (56)–(57)] are identical to those obtained in Paper I for HTI media due to a single set of rotationally invariant fractures. In principle, the inversion based on equations (54)–(57) requires knowledge of the squared velocity ratio $g = (V_S/V_P)^2$ that cannot be determined without shear- or converted-wave data. However, numerical tests in Paper I show that even a relatively rough estimate of g is sufficient for recovering the weaknesses with acceptable accuracy.

	Δ_{N1}	Δ_{T1}	Δ_{N2}	Δ_{T2}
Actual	0.30	0.15	0.60	0.30
Estimated	0.28	0.14	0.66	0.21
Actual	0.30	0.15	0	0
Estimated	0.30	0.14	0	0
Actual	0	0	0.60	0.30
Estimated	0	0	0.67	0.21

Table 1. Comparison of the actual fracture parameters with those estimated by inverting the exact anisotropic coefficients [equations (32)–(34) and Appendix B] using the linearized equations (54)–(57); the squared velocity ratio $g = 0.25$. The first model (top row) is composed of two orthogonal fracture sets in an isotropic background, while the second and third models contain only one fracture set (i.e., they have the HTI symmetry).

To test the accuracy of the weak-anisotropy approximations (54)–(57), we computed the exact anisotropic coefficients $\delta^{(1,2)}$ and $\eta^{(1,2)}$ for three fractured models in Table 1 [using equations (32)–(34) and the definitions from Appendix B] and inverted them for the weaknesses in the limit of weak anisotropy. Table 1 shows that the approximations (54)–(57) give reasonably good estimates of the fracture weaknesses. The only noticeable error, in the tangential weakness of the second fracture set, is not associated with the influence of the first set because it remains the same for the corresponding HTI model (third row in Table 1).

P- and PS-wave traveltimes

If dipping events are not available and common-midpoint spreads are not sufficiently long for using nonhyperbolic moveout, it may be possible to find all fracture weaknesses by combining P- and PS-wave data. Similar to pure modes, the azimuthally varying NMO velocity of the PS-wave in a horizontal orthorhombic layer is described by an ellipse aligned with the vertical symmetry planes (Grechka et al., 1999). The semi-axes of the P- and two split PS-wave NMO ellipses (i.e., the symmetry-plane NMO velocities) can be used to reconstruct the NMO ellipses of the pure shear waves S_1 and S_2 using the formalism of Grechka et al. (1999). Assuming that the wave S_1 represents an SV (in-plane polarized) mode in the $[x_2, x_3]$-plane [subscript "(1)"], the semi-axes of the shear-wave ellipses can be written as

$$V^{(2)}_{S1,\mathrm{nmo}} = V_{S1}\sqrt{1+2\,\gamma^{(2)}} = V^{(1)}_{S2,\mathrm{nmo}}\,, \tag{58}$$

$$V^{(1)}_{S1,\mathrm{nmo}} = V_{S1}\sqrt{1+2\,\sigma^{(1)}}\,, \tag{59}$$

$$V^{(2)}_{S2,\mathrm{nmo}} = V_{S2}\sqrt{1+2\,\sigma^{(2)}}\,, \tag{60}$$

$$V^{(1)}_{S2,\mathrm{nmo}} = V_{S2}\sqrt{1+2\,\gamma^{(1)}} = V^{(2)}_{S1,\mathrm{nmo}}\,. \tag{61}$$

Here $\sigma^{(1)}$ and $\sigma^{(2)}$ are the anisotropic coefficients,

$$\sigma^{(1)} = \left(\frac{V_{P0}}{V_{S1}}\right)^2 (\epsilon^{(1)} - \delta^{(1)}), \tag{62}$$

$$\sigma^{(2)} \equiv \left(\frac{V_{P0}}{V_{S2}}\right)^2 (\epsilon^{(2)} - \delta^{(2)}), \tag{63}$$

and V_{S1} and V_{S2} are the vertical velocities of the split shear waves:

$$V_{S2} = V_{S0}, \tag{64}$$

$$V_{S1} = V_{S2}\sqrt{\frac{1+2\gamma^{(1)}}{1+2\gamma^{(2)}}}. \tag{65}$$

Including the P- and S-wave NMO and vertical velocities into the parameter-estimation procedure makes it possible to determine the squared vertical-velocity ratio g and six anisotropic coefficients - $\delta^{(1,2)}$, $\epsilon^{(1,2)}$ and $\gamma^{(1,2)}$. Since the anisotropic parameters depend on only four fracture weaknesses, the combination of P and PS provides useful redundancy in the inversion procedure. The weaknesses can be computed, for example, as

$$\Delta_{T1} = 1 - \left(\frac{V^{(2)}_{S1,\mathrm{nmo}}}{V_{S2}}\right)^2, \tag{66}$$

$$\Delta_{T2} = 1 - \left(\frac{V^{(1)}_{S2,\mathrm{nmo}}}{V_{S1}}\right)^2, \tag{67}$$

$$\Delta_{N1} = -\frac{1}{1-2\,g}\left[\Delta_{T1} + \frac{\delta^{(2)}}{2\,g}\right], \tag{68}$$

$$\Delta_{N2} = -\frac{1}{1-2\,g}\left[\Delta_{T2} + \frac{\delta^{(1)}}{2\,g}\right]. \tag{69}$$

Discussion and conclusions

Applying the linear slip theory developed by Schoenberg (1980, 1983), we studied two types of orthorhombic media believed to be typical for naturally fractured reservoirs. The first model contains a single set of vertical fractures embedded in a VTI background (e.g., the background anisotropy may be due to fine layering) while the second is produced by two orthogonal systems of rotationally invariant fractures in an isotropic host rock. For both effective models we obtained Tsvankin's (1997b) anisotropic parameters, which capture the combinations of the stiffness coefficients responsible for commonly measured seismic signatures.

To gain a better understanding of the influence of fractures on the effective medium, we simplified the anisotropic parameters under the assumption of weak background and fracture-induced anisotropy. For the model with a single fracture set, the anisotropic coefficients of the HTI medium due to the fractures are simply added to the background parameters to produce the linearized effective parameters of the orthorhombic medium. Therefore, subtracting the effective coefficients defined in the vertical symmetry planes eliminates the influence of the background and reduces the inverse problem to that for horizontal transverse isotropy (Paper I). The information necessary for this inversion procedure can be obtained from the azimuthally dependent P-wave reflection traveltimes alone, if dipping events or nonhyperbolic moveout are available (also, it is necessary to have an estimate of P- and S-wave vertical velocities). Alternatively, the inversion can be performed by combining the P-wave NMO ellipse from a horizontal reflector with other data, such as the azimuthally varying P-wave AVO gradient or the vertical traveltimes and, possibly, NMO velocities of the split converted (PS) modes. The algorithm based on the NMO ellipses and AVO gradients of P- and PS-waves reflected from horizontal interfaces coincides with that outlined in Paper I for HTI media (i.e., it is independent of the presence of anisotropy in the background).

In the case of two orthogonal fracture sets, the linearized expressions for the effective anisotropic coefficients in each vertical symmetry plane contain only the contribution of the fractures orthogonal to this plane. As a result, the inversion for the fracture weaknesses splits into two separate inversion procedures in the symmetry planes which can be carried out using the HTI algorithm of Paper I. In contrast to the model with a single fracture set, however, determination of the weaknesses of both fracture sets requires knowledge of the vertical velocities in addition to the azimuthally varying surface seismic signatures. The inversion procedure for this model may also be based entirely on P-wave reflection traveltimes, if the data contain dipping events or nonhyperbolic moveout; otherwise, it is necessary to combine P- and PS-wave NMO velocities from horizontal reflectors.

Although both effective media considered in the paper have orthorhombic symmetry, the results of our analysis indicate several possible ways to identify the correct underlying physical model. Since in both cases the stiffness tensor is described by fewer independent parameters then for general orthorhombic media, the anisotropic coefficients satisfy several constraints, which are different for the models with one and two fracture sets. Another useful criterion is the sign of the anisotropic parameters. The coefficients $\epsilon^{(1,2)}$, $\delta^{(1,2)}$, and $\gamma^{(1,2)}$ for the model with two orthogonal systems of fractures in an isotropic background are always *negative* [equations (41)–(43) and (45)–(47)]. In contrast, the anisotropic coefficients ϵ, and γ (and often δ as well) defined in the fracture plane of the model with a single fracture set in a VTI

background are usually *positive*. Also, we can distinguish between the two models by comparing the polarization direction of the vertically traveling fast shear wave with the orientation of the semi-major axis of the P-wave NMO ellipse. For one set of fractures (in either isotropic or VTI background), they always coincide with each other, whereas for two systems of fractures with different fluid content they may become orthogonal. This happens, for example, if the two inequalities $\Delta_{T1} > \Delta_{T2}$ and $(1-2g)\Delta_{N1} + \Delta_{T1} < (1-2g)\Delta_{N2} + \Delta_{T2}$ (or, equivalently, $\delta^{(2)} > \delta^{(1)}$) are satisfied simultaneously.

Acknowledgments

This research was carried out during a visit of Andrey Bakulin to the Center for Wave Phenomena (CWP) at the Colorado School of Mines in the Fall of 1998. We are grateful to members of the A(nisotropy)-team of CWP for helpful discussions. The support for this work was provided by the members of the Consortium Project on Seismic Inverse Methods for Complex Structures at CWP and by the United States Department of Energy (award #DE-FG03-98ER14908).

References

Al-Dajani, A., Tsvankin, I., and Toksöz, N., 1998, Nonhyperbolic reflection moveout in azimuthally anisotropic media: 68th Ann. Internat. Mtg., Soc. Expl. Geophys., Expanded Abstracts, 1479–1482.

Alkhalifah, T., and Tsvankin, I., 1995, Velocity analysis in transversely isotropic media: Geophysics, **60**, 1550–1566.

Bakulin, A.V., Grechka, V., and Tsvankin, I., 1999, Estimation of fracture parameters from reflection seismic data. Part I: HTI model due to a single fracture set: this volume (Paper I).

Bakulin, A.V., and Molotkov, L.A., 1998, Effective models of fractured and porous media: St.Petersburg University Press (in Russian).

Grechka, V., and Tsvankin, I., 1998, 3-D description of normal moveout in anisotropic media: Geophysics, **63**, 1079–1092.

Grechka, V., and Tsvankin, I., 1999a, 3-D moveout inversion in azimuthally anisotropic media with lateral velocity variation: Theory and case study: Geophysics, in press.

Grechka, V., and Tsvankin, I., 1999b, Moveout velocity analysis and parameter estimation in orthorhombic media: Geophysics, in press.

Grechka, V., Theophanis, S., and Tsvankin, I., 1999, Joint inversion of P- and PS-waves in orthorhombic media: Theory and a physical-modeling study: Geophysics, **64**, 146–161.

Hudson, J.A., 1980, Overall properties of a cracked solid: Math. Proc. Camb. Phil. Soc., **88**, 371–384.

Hudson, J.A., 1981, Wave speeds and attenuation of elastic waves in material containing cracks: Geophys. J. Roy. Astr. Soc., **64**, 133–150.

Hudson, J.A., 1988, Seismic wave propagation through material containing partially saturated cracks: Geophys. J., **92**, 33–37.

Lynn, H.B., Simon, K.M., Bates, C.R., and van Dok, R., 1996, Azimuthal anisotropy in P-wave 3-D (multiazimuth) data: The Leading Edge, **15**, 923–928.

Martin, M.A., Davis, T.L., 1987, Shear-wave birefringence: A new tool for evaluating fractured reservoirs: The Leading Edge, **6**, 22–28.

Molotkov, L.A., and Bakulin, A.V., 1997, An effective model of a fractured medium with fractures modeled by the surfaces of discontinuity of displacements: Journal of Mathematical Sciences, **86**, No 3, 2735–2746.

Mueller, M.C., 1991, Prediction of lateral variability in fracture intensity using multicomponent shear-wave surface seismic as a precursor to horizontal drilling in Austin chalk: Geophys. J. Int., **107**, 409–415.

Nichols, D., Muir, F., and Schoenberg, M., 1989, Elastic properties of rocks with multiple sets of fractures: 59th Ann. Internat. Mtg., Soc. Expl. Geophys., Expanded Abstracts, 471–474.

Rüger, A., and Tsvankin, I., 1997, Using AVO for fracture detection: Analytic basis and practical solutions: The Leading Edge, **10**, 1429–1434.

Rüger, A., 1997, P-wave reflection coefficients for transversely isotropic models with vertical and horizontal axis of symmetry: Geophysics, **62**, 713–722.

Rüger, A., 1998, Variation of P-wave reflectivity with offset and azimuth in anisotropic media: Geophysics, **63**, 935–947.

Schoenberg, M., 1980, Elastic wave behavior across linear slip interfaces: J. Acoust. Soc. Am., **68**, 1516–1521.

Schoenberg, M., 1983, Reflection of elastic waves from periodically stratified media with interfacial slip: Geophys. Prosp., **31**, 265–292.

Schoenberg, M., and Douma, J., 1988, Elastic wave propagation in media with parallel fractures an aligned cracks: Geophys. Prosp., **36**, 571–590.

Schoenberg, M., and Helbig, K., 1997, Orthorhombic media: Modeling elastic wave behavior in a vertically fractured earth: Geophysics, **62**, 1954–1974.

Schoenberg, M., and Muir, F., 1989, A calculus for finely layered anisotropic media: Geophysics, **54**, 581–589.

Schoenberg, M., and Sayers, C., 1995, Seismic anisotropy of fractured rock: Geophysics, **60**, 204–211.

Thomsen, L., 1986, Weak elastic anisotropy: Geophysics, **51**, 1954–1966.

Thomsen, L., 1995, Elastic anisotropy due to aligned cracks in porous rock: Geophys. Prosp., **43**, 805–830.

Tsvankin, I., 1997a, Reflection moveout and parameter estimation for horizontal transverse isotropy: Geophysics, **62**, 614 –629.

Tsvankin, I., 1997b, Anisotropic parameters and P-wave velocity for orthorhombic media: Geophysics, **62**, 1292–1309.

Winterstein, D.F., 1990, Velocity anisotropy terminology for geophysicists: Geophysics, **55**, 1070–1088.

Withers, R., and Corrigan, D., 1997, Fracture detection using wide azimuth 3D seismic surveys: 59th EAGE Conference, Geneva, Extended Abstracts, Paper E003.

APPENDIX A: Compliance formalism for fractured media

Here we briefly review both exact and approximate methods of obtaining effective parameters of fractured media using the results of Schoenberg (1980, 1983), Schoenberg and Douma (1988), Schoenberg and Muir (1989), Nichols et al. (1989), and Molotkov and Bakulin (1997). A more detailed discussion of different approaches to effective medium theory for fractured models can be found in Paper I.

It is simpler to determine the effective elastic parameters of fractured media by using the compliances $\mathbf{s}$ instead of the stiffnesses $\mathbf{c}$. The effective compliance matrix of a fractured medium can be written as the sum of the background compliance $\mathbf{s}_b$ and the so-called matrix of excess fracture compliance $\mathbf{s}_f$:

$$\mathbf{c}^{-1} \equiv \mathbf{s} = \mathbf{s}_b + \mathbf{s}_f. \tag{A1}$$

If the background is transversely isotropic with a vertical symmetry axis (VTI), the matrix $\mathbf{s}_b$ is given by

$$\mathbf{c}_b \equiv \mathbf{s}_b^{-1} = \begin{pmatrix} c_{11b} & c_{12b} & c_{13b} & 0 & 0 & 0 \\ c_{12b} & c_{11b} & c_{13b} & 0 & 0 & 0 \\ c_{13b} & c_{13b} & c_{33b} & 0 & 0 & 0 \\ 0 & 0 & 0 & c_{44b} & 0 & 0 \\ 0 & 0 & 0 & 0 & c_{44b} & 0 \\ 0 & 0 & 0 & 0 & 0 & c_{66b} \end{pmatrix}, \tag{A2}$$

where $c_{12b} = c_{11b} - 2\,c_{66b}$. The matrix $\mathbf{s}_f$ of the excess compliance of a fracture set with the normal parallel to the x_1-axis can be written as

$$\mathbf{s}_f = \begin{pmatrix} K_N & 0 & 0 & 0 & 0 & 0 \\ 0 & 0 & 0 & 0 & 0 & 0 \\ 0 & 0 & 0 & 0 & 0 & 0 \\ 0 & 0 & 0 & 0 & 0 & 0 \\ 0 & 0 & 0 & 0 & K_V & 0 \\ 0 & 0 & 0 & 0 & 0 & K_H \end{pmatrix}, \tag{A3}$$

where K_N is the normal fracture compliance, and K_V and K_H are the two shear compliances in the vertical and horizontal directions. The matrix $\mathbf{s}_f$ in equation (A3) is assumed to be diagonal, which is not necessarily the case if the fractures are corrugated (Paper I). Since $K_V \neq K_H$, fractures described by the matrix (A3) are sometimes called "orthorhombic" (Schoenberg and Douma, 1988).

It is convenient to replace the excess fracture compliances K_N, K_V, and K_H by the following dimensionless quantities introduced by Schoenberg and Helbig (1997):

$$\Delta_N = \frac{K_N\, c_{11b}}{1 + K_N\, c_{11b}}, \qquad \Delta_V = \frac{K_V\, c_{44b}}{1 + K_V\, c_{44b}}, \qquad \Delta_H = \frac{K_H\, c_{66b}}{1 + K_H\, c_{66b}}. \tag{A4}$$

Then equation (A3) becomes

$$\mathbf{s}_f = \begin{pmatrix} \frac{\Delta_N/c_{11b}}{1-\Delta_N} & 0 & 0 & 0 & 0 & 0 \\ 0 & 0 & 0 & 0 & 0 & 0 \\ 0 & 0 & 0 & 0 & 0 & 0 \\ 0 & 0 & 0 & 0 & 0 & 0 \\ 0 & 0 & 0 & 0 & \frac{\Delta_V/c_{44b}}{1-\Delta_V} & 0 \\ 0 & 0 & 0 & 0 & 0 & \frac{\Delta_H/c_{66b}}{1-\Delta_H} \end{pmatrix}. \tag{A5}$$

We will call Δ_N, Δ_V, Δ_H the normal, vertical and horizontal *weaknesses* introduced by the fractures (Bakulin and Molotkov, 1998). The weaknesses vary from 0 to 1, with the zero value corresponding to unfractured media and unity describing heavily fractured media in which the P- (for $\Delta_N = 1$) or S-wave (for $\Delta_V = 1$ or $\Delta_H = 1$) velocity vanishes for propagation across the fractures (Paper I).

Substituting equations (A2) and (A5) into equation (A1) yields the effective stiffness matrix for a single fracture set embedded in a VTI background (Schoenberg and Helbig, 1997):

$$\mathbf{c} = \begin{pmatrix} \tilde{\mathbf{c}}_1 & \mathbf{0} \\ \mathbf{0} & \tilde{\mathbf{c}}_2 \end{pmatrix}, \tag{A6}$$

where

$$\tilde{\mathbf{c}}_1 = \begin{pmatrix} c_{11b}\,\ell & c_{12b}\,\ell & c_{13b}\,\ell \\ c_{12b}\,\ell & c_{11b} - \wp_1 & c_{13b} - \wp_2 \\ c_{13b}\,\ell & c_{13b} - \wp_2 & c_{33b} - \wp_3 \end{pmatrix}, \tag{A7}$$

$$\tilde{\mathbf{c}}_2 = \begin{pmatrix} c_{44b} & 0 & 0 \\ 0 & c_{44b}\,(1-\Delta_V) & 0 \\ 0 & 0 & c_{66b}\,(1-\Delta_H) \end{pmatrix}, \tag{A8}$$

$\ell = 1 - \Delta_N$, $\wp_1 = \Delta_N\, c_{12b}^2/c_{11b}$, $\wp_2 = \Delta_N\, c_{12b}\, c_{13b}/c_{11b}$, $\wp_3 = \Delta_N\, c_{13b}^2/c_{11b}$, and $\mathbf{0}$ is the 3×3 zero matrix.

Alternatively, the same result can be obtained using

the series

$$\begin{aligned}\mathbf{c} \equiv [\mathbf{s}_b + \mathbf{s}_f]^{-1} &= [(\mathbf{I} + \mathbf{s}_f\, {\mathbf{s}_b}^{-1})\, \mathbf{s}_b]^{-1} \\ &= \mathbf{c}_b [\mathbf{I} + \mathbf{s}_f\, \mathbf{c}_b]^{-1} \\ &= \mathbf{c}_b \sum_{k=0}^{\infty} (-\mathbf{s}_f\, \mathbf{c}_b)^k\,, \end{aligned} \tag{A9}$$

where $\mathbf{I}$ is the 6×6 identity matrix. The series (A9) converges to (A6) if all eigenvalues of the matrix $\mathbf{s}_f \mathbf{c}_b$ have absolute values less than 1. This is always the case if the weaknesses Δ_N, Δ_V, Δ_H, which define nonzero eigenvalues of the matrix $\mathbf{s}_f$ [see equation (A5)], are sufficiently small.

Equation (A9) can serve as the basis for developing useful approximations for the effective stiffness matrix $\mathbf{c}$. If the crack density (or fracture intensity) is small, and the weaknesses $\{\Delta_N, \Delta_V, \Delta_H\} \ll 1$, we may truncate the series (A9) by keeping only linear terms with respect to Δ_N, Δ_V, and Δ_H:

$$\mathbf{c} \approx \mathbf{c}_b - \mathbf{c}_b\, \mathbf{s}_f\, \mathbf{c}_b\,. \tag{A10}$$

It is interesting to note that equation (A10) becomes *exact* if we replace the matrix $\mathbf{s}_f$ [equation (A5)] by its linearized version

$$\mathbf{s}_f^{\rm lin} = \begin{pmatrix} \frac{\Delta_N}{c_{11\,b}} & 0 & 0 & 0 & 0 & 0 \\ 0 & 0 & 0 & 0 & 0 & 0 \\ 0 & 0 & 0 & 0 & 0 & 0 \\ 0 & 0 & 0 & 0 & 0 & 0 \\ 0 & 0 & 0 & 0 & \frac{\Delta_V}{c_{44\,b}} & 0 \\ 0 & 0 & 0 & 0 & 0 & \frac{\Delta_H}{c_{66\,b}} \end{pmatrix}. \tag{A11}$$

The approximation (A10) can be used to obtain two important results. First, it can be extended in a straightforward way to multiple fracture sets (Nichols et al., 1989). If the effective compliance represents the sum of the excess compliances of N fracture sets,

$$\mathbf{s} = \sum_{i=1}^{N} \mathbf{s}_{fi}\,, \tag{A12}$$

then for the effective stiffness $\mathbf{c}$ we have

$$\mathbf{c} \approx \mathbf{c}_b - \sum_{i=1}^{N} \mathbf{c}_b\, \mathbf{s}_{fi}\, \mathbf{c}_b\,. \tag{A13}$$

Note that the compliance matrix $\mathbf{s}_{fi}$ cannot be described by equation (A3) if the normal $\mathbf{n}_i$ to the ith fracture set does not coincide with the x_1-axis. The matrices $\mathbf{s}_{fi}$ for arbitrary orientation of $\mathbf{n}_i$ may be obtained from equation (A3) using the so-called Bond rotation (Winterstein, 1990). For example, the compliance matrix for a fracture set with the normal $\mathbf{n}_i = [0, 1, 0]$ has the form

$$\mathbf{s}_{fi} = \begin{pmatrix} 0 & 0 & 0 & 0 & 0 & 0 \\ 0 & K_N & 0 & 0 & 0 & 0 \\ 0 & 0 & 0 & 0 & 0 & 0 \\ 0 & 0 & 0 & K_V & 0 & 0 \\ 0 & 0 & 0 & 0 & 0 & 0 \\ 0 & 0 & 0 & 0 & 0 & K_H \end{pmatrix}. \tag{A14}$$

Second, equation (A10) is well-suited for deriving the weak-anisotropy approximation for the stiffnesses of effective media formed by fractures embedded in an anisotropic background. We assume that the background medium is weakly anisotropic, so that

$$\mathbf{c}_b = \mathbf{c}_b^{\rm iso} + \varepsilon\, \mathbf{c}_b^{\rm ani}\,, \tag{A15}$$

where $\mathbf{c}_b^{\rm iso}$ is the stiffness matrix of a purely isotropic solid that approximates $\mathbf{c}_b$ in some sense, $\mathbf{c}_b^{\rm ani}$ is the "anisotropic" portion of $\mathbf{c}_b$, and $\varepsilon \ll 1$. We also assume that the elements of the fracture compliance matrix are of the same order as ε and can be denoted as $\varepsilon \mathbf{s}_f$. If we represent the effective stiffness matrix $\mathbf{c}$ in the form similar to equation (A15), equation (A10) can be rewritten as

$$\begin{aligned}\mathbf{c}^{\rm iso} + \varepsilon\, \mathbf{c}^{\rm ani} \approx\ & \mathbf{c}_b^{\rm iso} + \varepsilon\, \mathbf{c}_b^{\rm ani} \\ & - \left(\mathbf{c}_b^{\rm iso} + \varepsilon\, \mathbf{c}_b^{\rm ani}\right) \varepsilon\, \mathbf{s}_f\, \left(\mathbf{c}_b^{\rm iso} + \varepsilon\, \mathbf{c}_b^{\rm ani}\right). \end{aligned} \tag{A16}$$

Collecting the terms linear in ε yields

$$\mathbf{c}^{\rm ani} = \mathbf{c}_b^{\rm ani} - \mathbf{c}_b^{\rm iso}\, \mathbf{s}_f\, \mathbf{c}_b^{\rm iso}\,. \tag{A17}$$

This equation, valid in the weak-anisotropy limit, can be loosely interpreted in the following way: the anisotropy $\mathbf{c}^{\rm ani}$ of an effective medium containing fractures in an anisotropic background described by $\mathbf{c}_b$ is equal to the sum of the background anisotropy $\mathbf{c}_b^{\rm ani}$ and the anisotropy caused by the fractures embedded into any isotropic medium with $\mathbf{c}_b^{\rm iso}$ sufficiently close to $\mathbf{c}_b$ (i.e., $\mathbf{c}_b^{\rm iso}$ has to satisfy the inequality $\left| \frac{||\mathbf{c}_b||}{||\mathbf{c}_b^{\rm iso}||} - 1 \right| < \varepsilon$).

APPENDIX B: Anisotropic parameters for orthorhombic media

The basic set of the anisotropic parameters for orthorhombic media was introduced by Tsvankin (1997b). His notation contains the vertical velocities of the P-wave and one of the S-waves and seven dimensionless Thomsen-type (1986) anisotropic coefficients. The definitions of those parameters in terms of the stiffnesses c_{ij} and density ρ are given below.

- V_{P0} – the P-wave vertical velocity:

$$V_{P0} \equiv \sqrt{c_{33}/\rho} \qquad (\rho \text{ is the density}). \tag{B1}$$

- V_{S0} – the vertical velocity of the S-wave polarized in the x_1-direction:

$$V_{S0} \equiv \sqrt{c_{55}/\rho}\,. \tag{B2}$$

- $\epsilon^{(2)}$ – the VTI parameter ϵ in the $[x_1, x_3]$ symmetry plane normal to the x_2-axis (this explains the superscript "2"):

$$\epsilon^{(2)} \equiv \frac{c_{11} - c_{33}}{2\,c_{33}}\,. \tag{B3}$$

- $\delta^{(2)}$ – the VTI parameter δ in the $[x_1, x_3]$ plane:

$$\delta^{(2)} \equiv \frac{(c_{13} + c_{55})^2 - (c_{33} - c_{55})^2}{2\,c_{33}\,(c_{33} - c_{55})}\,. \tag{B4}$$

- $\gamma^{(2)}$ – the VTI parameter γ in the $[x_1, x_3]$ plane :

$$\gamma^{(2)} \equiv \frac{c_{66} - c_{44}}{2\,c_{44}}\,. \tag{B5}$$

- $\epsilon^{(1)}$ – the VTI parameter ϵ in the $[x_2, x_3]$ symmetry plane:

$$\epsilon^{(1)} \equiv \frac{c_{22} - c_{33}}{2\,c_{33}}\,. \tag{B6}$$

- $\delta^{(1)}$ – the VTI parameter δ in the $[x_2, x_3]$ plane:

$$\delta^{(1)} \equiv \frac{(c_{23} + c_{44})^2 - (c_{33} - c_{44})^2}{2\,c_{33}\,(c_{33} - c_{44})}\,. \tag{B7}$$

- $\gamma^{(1)}$ – the VTI parameter γ in the $[x_2, x_3]$ plane:

$$\gamma^{(1)} \equiv \frac{c_{66} - c_{55}}{2\,c_{55}}\,. \tag{B8}$$

- $\delta^{(3)}$ – the VTI parameter δ in the $[x_1, x_2]$ plane (x_1 plays the role of the symmetry axis):

$$\delta^{(3)} \equiv \frac{(c_{12} + c_{66})^2 - (c_{11} - c_{66})^2}{2\,c_{11}\,(c_{11} - c_{66})}\,. \tag{B9}$$

These nine parameters fully describe wave propagation in general orthorhombic media. In particular applications, however, it is convenient to operate with specific combinations of Tsvankin's parameters. For example, P-wave NMO velocity from dipping reflectors depends on three coefficients η, which determine the anellipticity of the P-wave slowness in the symmetry planes (Grechka and Tsvankin, 1999b). The definitions of $\eta^{(1,2,3)}$ are analogous to that of Alkhalifah-Tsvankin (1995) coefficient η in VTI media:

- $\eta^{(1)}$ – the VTI parameter η in the $[x_2, x_3]$ plane:

$$\eta^{(1)} \equiv \frac{\epsilon^{(1)} - \delta^{(1)}}{1 + 2\,\delta^{(1)}}\,. \tag{B10}$$

- $\eta^{(2)}$ – the VTI parameter η in the $[x_1, x_3]$ plane:

$$\eta^{(2)} \equiv \frac{\epsilon^{(2)} - \delta^{(2)}}{1 + 2\,\delta^{(2)}}\,. \tag{B11}$$

- $\eta^{(3)}$ – the VTI parameter η in the $[x_1, x_2]$ plane:

$$\eta^{(3)} \equiv \frac{\epsilon^{(1)} - \epsilon^{(2)} - \delta^{(3)}(1 + 2\,\epsilon^{(2)})}{(1 + 2\,\epsilon^{(2)})(1 + 2\,\delta^{(3)})}\,. \tag{B12}$$

Vertical transverse isotropy may be considered as a special case of orthorhombic media where

$$\epsilon^{(1)} = \epsilon^{(2)} = \epsilon\,, \tag{B13}$$

$$\delta^{(1)} = \delta^{(2)} = \delta\,, \tag{B14}$$

$$\gamma^{(1)} = \gamma^{(2)} = \gamma\,, \tag{B15}$$

$$\delta^{(3)} = 0\,, \tag{B16}$$

and, as a consequence,

$$\eta^{(1)} = \eta^{(2)} = \eta\,, \tag{B17}$$

$$\eta^{(3)} = 0\,. \tag{B18}$$

APPENDIX C: Two identical fracture sets

If the model includes two identical orthogonal fracture sets in a purely isotropic background, only four effective stiffnesses out of nine remain independent because the stiffness matrix depends on four quantities: λ, μ, $\Delta_{N1} = \Delta_{N2} \equiv \Delta_N$ and $\Delta_{T1} = \Delta_{T2} \equiv \Delta_T$. From equations (32)–(35) it follows that in this case $c_{11} = c_{22}$, $c_{13} = c_{23}$, and $c_{44} = c_{55}$. The constraints (39) and (40) become identical and, together with (38), may be reduced to

$$c_{12}\,(c_{33} + c_{13}) = c_{13}\,(c_{11} + c_{13}) \tag{C1}$$

and

$$2\,(c_{11} + c_{13})\;c_{44}\,c_{66} = (2\,c_{66} - c_{44})\left(c_{11}\,c_{33} - c_{13}^2\right)\,. \tag{C2}$$

We can call this medium "quasi-VTI" because its stiffness matrix is close to the one for vertical transverse isotropy. Unlike real VTI media, however, the stiffnesses of the quasi-VTI model satisfy the constraints (C1) and (C2) which replace the VTI relationship $c_{11} = c_{12} + 2\,c_{66}$. Physically, the model with two identical fracture sets does not have the VTI symmetry due to the difference between the normal and shear compliances. Indeed, the combination of the stiffnesses that has to vanish in VTI media can be written in the exact form as

$$c_{11} - 2\,c_{66} - c_{12} = \frac{4\,\mu^2\,(K_T - K_N)}{(1 + 2\,\mu\,K_N)(1 + 2\,\mu\,K_T)}\,. \tag{C3}$$

The anisotropic coefficients of quasi-VTI media are described by equations (B3)–(B5), (B13)–(B15), and

$$\delta^{(3)} = -\,\frac{4\,\mu^2\,(\lambda + \mu)\,(K_T - K_N)}{2\,\mu + \lambda/[1 + 2\,(\lambda + \mu)\,K_N]} \times \left(\mu + 2\,\mu\,(\lambda + \mu)\,(K_T - K_N) + \frac{\lambda\,(1 + 4\,\mu\,K_N)}{1 + 2\,\mu\,K_N} + 2\,\mu^2\,K_T\,\frac{1 + 2\,(\lambda + \mu)\,K_N}{1 + 2\,\mu\,K_N}\right)^{-1}\,. \tag{C4}$$

It is interesting to note that quasi-VTI media have two additional vertical symmetry planes at 45° with respect to the planes $[x_1, x_3]$ and $[x_2, x_3]$. Expressions for anisotropic coefficients $\epsilon^{(1,2)}$, $\delta^{(1,2)}$, and $\gamma^{(1,2)}$ which could be

defined within these symmetry planes are different from those given by equations (41)–(50).

Two identical "scalar" fracture sets

If we further assume that both fracture sets are filled with gas (i.e., $K_N = K_T$; Schoenberg and Sayers, 1995; Paper I), the effective medium becomes VTI. The effective stiffnesses given below depend only on the background parameters λ and μ and the weakness $\Delta_T = \frac{K_T\,\mu}{1+K_T\,\mu}$ [equation (37)]:

$$c_{11} = (\lambda + 2\,\mu)\,\frac{(1-\Delta_T)(1+\Delta_T\,(3-4\,g))}{D}\,, \tag{C5}$$

$$c_{13} = \lambda\,\frac{1-\Delta_T^2}{D}\,, \tag{C6}$$

$$c_{33} = (\lambda + 2\,\mu)\,\frac{1-\Delta_T\,(8\,g-5)}{D}\,, \tag{C7}$$

$$c_{44} = \mu\,(1-\Delta_T)\,, \tag{C8}$$

$$c_{66} = \mu\,\frac{1-\Delta_T}{1+\Delta_T}\,, \tag{C9}$$

where

$$D \equiv (1+\Delta_T)[1+\Delta_T\,(2-3g)]\,. \tag{C10}$$

The five stiffness elements of this three-parametric VTI medium are related by two constraints that can be obtained by substituting the relation $c_{11} = c_{12} + 2\,c_{66}$ into equations (C1) and (C2). In terms of Thomsen's (1986) anisotropic coefficients, these constraints take the form

$$\epsilon = \delta = 4\,\gamma\,(1+2\,\gamma)(1-g)\,. \tag{C11}$$

The equality $\epsilon = \delta$ indicates that the effective medium is elliptically anisotropic. In the weak anisotropy limit, equation (C11) yields

$$\epsilon = \delta \approx 4\,\gamma\,(1-g)\,. \tag{C12}$$

For a typical value $g = 0.25$, $\epsilon = \delta \approx 3\,\gamma$.

APPENDIX D: Fracture characterization for two orthogonal fracture sets: special cases

Azimuthally independent *P*-wave NMO velocity

In contrast to the case of a single fracture set in an isotropic or VTI background, the orientation of two orthogonal fracture systems cannot always be found from the P-wave NMO ellipse from a horizontal reflector. If $\delta^{(1)} = \delta^{(2)}$ or, equivalently,

$$(1-2\,g)\,\Delta_{N1} + \Delta_{T1} = (1-2\,g)\,\Delta_{N2} + \Delta_{T2} \tag{D1}$$

[equations (42) and (46)], the P-wave NMO ellipse degenerates into a circle. This equation does not necessarily imply that the two systems of fractures are identical because it can be satisfied for fracture sets with different crack density (e.g., $\Delta_{T1} > \Delta_{T2}$) and different fluid saturation ($\Delta_{N1} < \Delta_{N2}$). The azimuths of fractures in this case can be found from the shear-wave polarization directions or using P-wave reflections from dipping interfaces and/or the azimuthal variation of P-wave nonhyperbolic moveout.

Equal tangential weaknesses

If the tangential weaknesses are equal to each other ($\Delta_{T1} = \Delta_{T2}$), the anisotropic coefficients $\gamma^{(1)}$ and $\gamma^{(2)}$ also become identical [see equations (43) and (47)], and there is no shear-wave splitting at vertical incidence. Hence, the fracture orientation cannot be determined from shear-wave splitting. However, if the fracture sets have different normal weaknesses ($\Delta_{N1} \neq \Delta_{N2}$), the fracture azimuths can be found using P-wave NMO ellipses from a horizontal or a dipping reflector.

Identical fracture sets (quasi-VTI medium)

In the case of two identical orthogonal fracture sets, neither the P-wave NMO ellipse from a horizontal reflector (it degenerates into a circle because $\delta^{(1)} = \delta^{(2)}$) nor the shear-wave polarization directions ($\gamma^{(1)} = \gamma^{(2)}$, see Appendix C) can be used to detect the fracture orientation. Still, due to the fact that $\delta^{(3)}$ (or $\eta^{(3)}$) differs from zero, the orientation can be found from normal moveout of P waves reflected from dipping interfaces or from P-wave nonhyperbolic moveout. The rest of the inversion procedure is similar to that for the general case of two different fracture systems.

Despite the absence of shear-wave splitting in the vertical direction, S-waves can still be used for estimation of the fracture parameters. The wavefront of the slow shear-wave in quasi-VTI media always has cusps at 45° with respect to the symmetry planes $[x_1, x_3]$ and $[x_2, x_3]$ (Figure D1) if $c_{11} - 2\,c_{66} - c_{12} > 0$ (or, equivalently, $K_T > K_N$; see equation (C3) and Paper I]. This wavefront structure by itself can be used to identify the symmetry directions (and, therefore, the fracture strikes) if a sufficient number of azimuthal measurements is available. (Another option, as discussed above, is to use P-wave data.) Once those directions are found, we can use equations (58)–(65) for the NMO velocities of the S_1- and S_2-waves in the vertical symmetry planes and estimate fracture parameters based on equations (66) and (68). It is interesting that in quasi-VTI media the S-wave normal-moveout velocities from a horizontal reflector are defined, strictly speaking, *only* within the vertical symmetry planes because the shear-wave singularity makes the S-wave offset-traveltime curve non-differentiable in any other azimuth.

Identical gas-filled fracture sets (VTI medium)

Finally, if two identical fracture sets are gas-filled, the

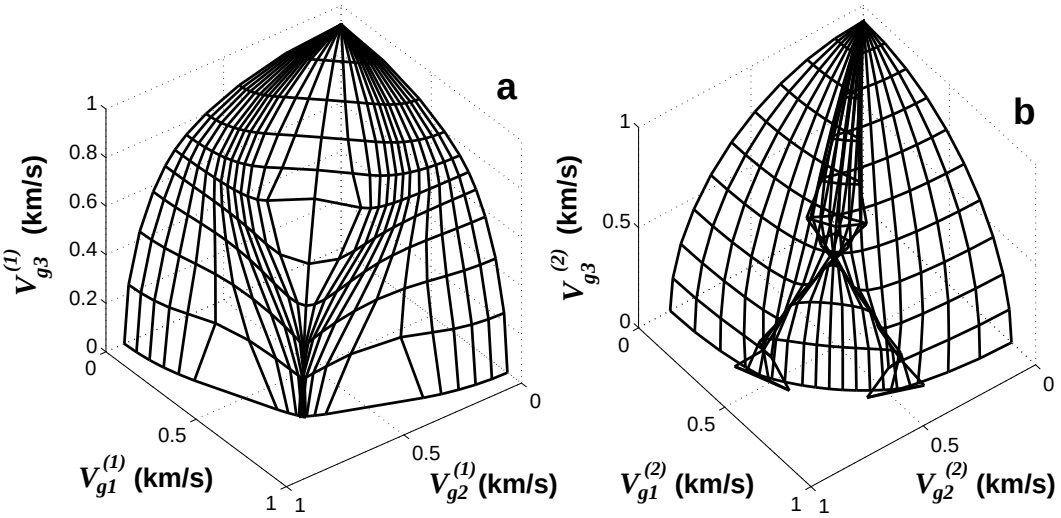

Figure D1. Group velocity surfaces of the fast (a) and slow (b) shear waves for the model with two identical orthogonal fracture sets.The background velocities are $V_P = 2$ km/s and $V_S = 1$ km/s. The fracture weaknesses $\Delta_N = 0$ and $\Delta_T = 0.15$ approximately correspond to fluid-filled penny-shaped cracks with a crack density of 7% . (Paper I).

effective medium becomes VTI (Appendix C). Since the VTI model is azimuthally isotropic, it is impossible to find the fracture orientation from seismic data. The single parameter Δ_T (or K_T) needed to describe the fractures may be found from any anisotropic coefficient given by equations (41)–(48) provided that the background V_S/V_P ratio is known. Estimating several anisotropic coefficients provides a redundancy that can be used to verify the validity of this model [see equation (C11)].